RSC Advances

This is an *Accepted Manuscript*, which has been through the Royal Society of Chemistry peer review process and has been accepted for publication.

Accepted Manuscripts are published online shortly after acceptance, before technical editing, formatting and proof reading. Using this free service, authors can make their results available to the community, in citable form, before we publish the edited article. This *Accepted Manuscript* will be replaced by the edited, formatted and paginated article as soon as this is available.

You can find more information about *Accepted Manuscripts* in the Information for Authors.

Please note that technical editing may introduce minor changes to the text and/or graphics, which may alter content. The journal's standard Terms & Conditions and the Ethical guidelines still apply. In no event shall the Royal Society of Chemistry be held responsible for any errors or omissions in this *Accepted Manuscript* or any consequences arising from the use of any information it contains.

ROYAL SOCIETY OF CHEMISTRY

www.rsc.org/advances

RSC Advances

RSCPublishing

ARTICLE

Establishment of a Long-Term Chick Forebrain Neuronal Culture on a Microelectrode Array Platform

Cite this: DOI: 10.1039/x0xx00000x

Received 00th January 2012,
Accepted 00th January 2012

DOI: 10.1039/x0xx00000x

www.rsc.org/

Serena Y. Kuang,[a] Ting Huang,[b] Zhonghai Wang,[c] Yongliang Lin[d], Mark Kindy[e], Tingfei Xi[b], and Bruce Z. Gao[c]

The biosensor system formed by culturing primary animal neurons on a microelectrode array (MEA) platform is drawing an increasing research interest for its power as a rapid, sensitive, functional neurotoxicity assessment, as well as for many other electrophysiological related research purposes. In this paper, we established a long-term chick forebrain neuron culture (C-FBN-C) on MEAs with a more than 5 month long lifespan and up to 5 month long stability in morphology and physiological function; characterized the C-FBN-C morphologically, functionally, and developmentally; partially compared its functional features with rodent counterpart; and discussed its pros and cons as a novel biosensor system in comparison to rodent counterpart and human induced pluripotent stem cells (hiPSCs). Our results show that C-FBN-C on MEA platform 1) can be used as a biosensor of its own type in a wide spectrum of basic biomedical research; 2) is of value in comparative physiology in cross-species studies; and 3) may have potential to be used as an alternative, cost-effective approach to rodent counterpart within shared common functional domains (such as specific types of ligand-gated ion channel receptors and subtypes expressed in the cortical tissues of both species) in large-scale environmental neurotoxicant screening that would otherwise require millions of animals.

Key words: microelectrode array, chick forebrain neuron, long-term culture, biosensor

[a] *William Beaumont School of Medicine, Oakland University, Rochester, MI 49309, USA. E-mail: kuang@oakland.edu*

[b] *Academy for Advanced Interdisciplinary Studies, Center for Biomedical Materials and Tissue Engineering, Peking University, Beijing, 100871, China.*

[c] *Department of Bioengineering, Clemson University, 201-5 Rhodes Research Hall, Clemson, SC 29634, USA.*

[d] *National Engineering Laboratory for Regenerative Implantable Medical Devices, Guangzhou, Guangdong 510530, China*

[e] *Departments of Neuroscience and Regenerative Medicine and Cell Biology, Medical University of South Carolina, Charleston, SC 29466, USA. E-mail: kingyms@musc.edu.*

Introduction

The coupling of rodent primary neuron culture with microelectrode array (MEA) technology results in a biosensor system that holds promise for use in rapid, sensitive, functional assessment of neuroactive agents and neurotoxicants and is thus considered "a physiologically-based neurotoxicity testing platform for the 21st century."[1] These neurons come mainly from rodent cortex, hippocampus, and spinal cord. Other types of neuron-based biosensors are in development but have not been well characterized, such as rodent dorsal root ganglion;[1] human embryonic stem cell-derived neuronal cells;[2] the NT-2 cell line derived from human pluripotent carcinoma stem cells;[3] chick spinal cord[4] and so on. The availability of the technology to generate human induced pluripotent stem cells (hiPSCs) from mature human cell sources[5] has great potential to provide a large supply of human neurons for neurotoxin assessment[6]. However, the current abilities in this field are still being developed. There are many challenges and costs associated with ensuring a consistent supply of useful hiPSCs, particularly in terms of reprogramming efficiency, differentiation reproducibility, and quality control. Recent and anticipated advances are expected to overcome these issues as innovative researchers continue to investigate and improve existing techniques and capabilities.

Using MEA technology, in the past, we explored a rarely used but abundant and economic cortical neuron source (i.e., embryonic chick forebrains, developed a chick forebrain neuron (FBN)-based biosensor on MEA, and characterized it partially and pharmacologically.[7] This novel biosensor system advanced our understanding about the functional features of cortical neuronal networks in vitro in two aspects. 1) Based on early patch clamp data on synapse formation and function in chick FBN culture (C-FBN-C),[8] we found that the synapse formation and function in vitro is much faster than in vivo, and there is a critical, narrow time window for the rapid early development of synapses. This narrow time window is potentially quite suitable for use in detecting chemicals that particularly influence the development of synapses. 2) The novel biosensor played an important role in comparative physiology. There was a more than half a century of debate about whether cell-type homologies of mammalian neocortex exist in a bird's brain. The debate was confirmed by a recent publication in PANS: neocortical cell type homologies are conserved from reptiles to mammals, and

RSC Advances Accepted Manuscript

these cells are organized into very different architectures in different species; they form cortical areas in reptiles, nuclei in birds, and cortical layers in mammals.[9] Based on this important finding, we provided a first line of in vitro functional data that support this finding: in comparison to rodent counterpart, the features of the spontaneous spiking activity (SSA) from chick FBN biosensor showed remarkable functional similarities in spatial and temporal firing pattern, tissue specificity in comparison to SSA pattern from spinal cord neurons, and responsiveness to selected classic neuroactive agents in terms of dose ranges used and EC_{50} (concentration that results in 50% of maximum response) for each agent.[7] The selected classic neuroactive agents include tetrodotoxin, a specific voltage-gated sodium channel blocker; verapamil, a specific voltage-gated L-type calcium channel blocker; Mg^{2+}, a NMDA channel blocker; NMDA, the prototype agonist of NMDA channels; APV, a specific NMDA channel antagonist; bicuculline, a specific $GABA_A$ type channel antagonist; and musimol, a specific $GABA_A$ channel agonist. Because of the shared drug responsiveness between mammals and birds, its application may be potentially extended as an alternative approach to rodent counterpart in neurotoxin-related testing in known shared receptor domains, especially for a large-scale screening of environmental neurotoxic chemicals, in terms of convenience and cost-effectiveness. Based on the work described above, the chick FBN biosensor shows its value to be used widely for research in the field of electrophysiology, neuroscience, biology, pharmacology, and neurotoxicology.

In this paper, we report details of how a long-term stable C-FBN-C is established on MEA platform to form the novel type C-FBN biosensor. In a previous publication, we 1) reported that C-FBN-Cs showed a remarkable embryonic-age-dependent culture morphology and lifespan when co-cultured with glial cells; 2) prolonged the in vitro lifespan of C-FBN-C from 14 days to 3 months; and 3) described how to acquire life-long, vigorous SSA from C-FBN-Cs.[10] In this paper, we optimized culture conditions, achieved a more than 5 month-long lifespan, characterized the C-FBN-C morphologically, functionally, and developmentally, and discussed its advantages and limitations in comparison to rodent counterpart, as well as hiPSCs-based MEA biosensor that may be seen in the near future.

Materials and methods

Cell culture

MEA preparation. Prior to forebrain dissection, surfaces of sterilized MEA chips (MCSMEA-S1-GR, 200/30ir-Ti with internal ground, MCS GmbH, Reutlingen, Germany) were activated using low oxygen plasma treatment (PDC-32G, Harrick) for 2-3 min. The chips were then coated with 0.05% polyethylenimine (PEI, P3143, Sigma) at 37° C overnight. Before dissociated cells were plated, chips were washed 4 times using sterilized deionized water. The chips were then covered with 500 µl serum-free Medium 199 (M199, M4530, Sigma) supplemented with 2% B27 (17504-044, Gibco) and 1% antibiotic/antimycotic (15240-062, Gibo) and kept in a typical cell-culture incubator at 37° C with 5% CO_2 and 95% humidity to balance the temperature and pH in preparation for plating.

Forebrain dissection and forebrain-cell dissociation. White Leghorn chick forebrains (Embryonic Day 8, 9, and 10 (E8-to-E10)) were dissected according to Heidemann et al.[11] Forebrain cells were then trypsinized (0.25% Trypsin, T4049, Sigma) for 5-7 min at 37° C before undergoing a few gentle titrations. The trypsin effect was deactivated by the addition of serum-containing medium, and the cell suspension was centrifuged at 1000 rpm for 5 min. Cell pellets were washed one more time using serum-free M199 and were re-suspended in the same medium for plating on MEA chips to record SSA or on glass-bottom culture dishes for immunostaining.

Cell plating and first-day culture: For MEA recording, cells were plated on MEA chips prepared as described above with 500 µl temperature- and pH-balanced medium at densities ranging from 1000 cells/mm^2 to 2500 cells/mm^2. The final total volume of medium on each MEA chip after cell plating was chosen to be 1000 µl. After plating, each MEA chip was covered with a sterilized Teflon® lid (ALAMEA-MEM5, ALA Scientific). SSA signals are very sensitive to osmotic fluctuation, and the Teflon lid, permeable to gases but not to water or bacteria,[12] helps minimize osmotic fluctuation in culture medium between medium changes. The covered MEA chips were placed in 100 mm petri dishes and held in a regular incubator (37° C, 5% CO_2, and 95% humidity) until the next day. For immunocytochemistry (ICC), cells were plated using the same medium on MatTek Corporation glass-bottom culture dishes (NC9344425, Fisher Scientific) with a plating density between 1000 and 2000 cells/mm^2 and cultured in the same incubator as the dishes containing MEAs.

Maintenance of long-term culture. Unlike our previous work using M199 with 10% fetal bovine serum ($M199^+$),[10] in this research Neurobasal® medium (NB, 21103-049, Gibco) was selected for cell culture and long-term maintenance. NB, originally designed with reduced osmolarity and reduced glutamate concentration to have excitatory neurotoxicity for serum-free culture of rodent embryonic cortical neurons,[13] was tested to explore whether this mammalian-suitable culture medium is also suitable for avian neurons. Since it was unknown whether serum-free NB would be suitable for C-FBN-Cs, both NB and NB supplemented with 2% FBS (NB^+) were tested. One day after cell plating, medium in half of the chips was changed to NB, and medium in the other half was changed to NB^+. Both NB and NB^+ groups were supplemented with 2% B27 (17504-044, Gibco) and 1% antibiotic/antimycotic (15240-062, Gibo) and kept in the same incubator. Thereafter, the interval (day in vitro, DIV) of medium change largely depended on cell density in culture. In general, 1/3 or 1/2 of the medium was changed (partial change) around 5 or 6 DIV in the first week and partially changed twice in the second week. No mitotic inhibitor was used to allow glial cells to cogrow with neurons because 1) we found that SSA signals were compromised to a greater or lesser degree even in the presence of a small dose of a mitotic inhibitor (e.g., Cytosine β-D-arabinofuranoside, Ara-C, C1768, Sigma) and 2) Ara-C compromised the integrity of C-FBN-Cs. Due to nonsuppressed glial proliferation, rapid culture metabolism, and the HEPES in NB, partial or full medium change was required every other day or every two days after two weeks, and every day after three weeks. While the medium-change frequency increased, particularly for cultures with a plating density near or higher than 2000 cells/mm^2 (usually during the second or third week), cultures required transfer to a low CO_2 (2.5%) incubator with conventional temperature and humidity (37° C and 95%). The partial pressure of CO_2 in this incubator was lowered by 0.5% every day until it reached 0%. Cultures were maintained at 0% CO_2 for several months with partial- or full-medium change every three days, every other day, or every day depending on visualized pH condition (color of the medium) in culture. No glial cell proliferation inhibitor was used; glial cells were co-cultured naturally with FBNs.

Immunocytochemistry

C-FBN-Cs at designated DIVs were fixed with 4% paraformaldehyde for 10 min at room temperature. A blocking buffer containing 0.05% Triton-X-100 in phosphorylated buffer saline (PBS) and 10% normal donkey serum (NDS, NC9624464) was used to permeate cell membranes and block nonspecific binding

RSC Advances Accepted Manuscript

 This journal is © The Royal Society of Chemistry 2015

sites for one h at room temperature. An antibody buffer (2% NDS in PBS) was used to dilute primary and secondary antibodies. The primary antibody was applied to cultures overnight at 4º C and washed in PBS 3 times for 5 min. The secondary antibody was applied to cultures for 1 h at room temperature and washed as before. Cultures were mounted with ProLong® Gold Antifade Reagent without DAPI (P36930, Molecular Probes). A Zeiss phase-contrast microscope or a Nikon confocal microscope was used to image the results of ICC. Targeted proteins included 1) microtubule associated protein2 (MAP2, a pan-neuronal marker and postsynaptic marker) and 2) glial fibrillary acidic protein (GFAP), a marker for astroglia. Primary antibodies were mouse anti-MAP2 (1:800, ab11267, Abcam) and rabbit-anti-GFAP (1:500, ab16997, Abcam). Secondary antibodies were Alexa fluoro 488-donkey anti-mouse IgG (1:200, A21202, Invitrogen) and Alexa fluro 594-donkey anti-rabbit IgG (1:200, A21207, Invitrogen).

MEA recording and data analysis

Methods of MEA recording and data analysis were described in our previous paper.[10] In brief, SSA signals were recorded using MEAs, amplified using MCS 1060-INV amplifier (MCS GmbH, Reutlingen, Germany), and collected using MC_Rack software (Version 4.3.0, MCS GmbH, Reutlingen, Germany) at a 25KHz sampling rate. MC_Rack extracted spike information simultaneously. A threshold of -7 times the standard deviation (SD) of the mean noise amplitude was set for spike detection in this study. Bursts were defined using the three criteria described in our previous paper[10] and detected using NeuroMEA, a MatLab-based program developed in our lab. NeuroMEA also created raster plots, which are commonly used with MEA data to present temporal and spatial features of SSA. To plot a raster plot, NeuroMEA allows a researcher to select active channels and the time window during which he/she wants to focus and show MEA signals. NeuroMEA then aligns selected active channels in rows and plots the time stamp of each spike that appears on each selected active channel within a pre-designated time window. The alignment of rows of active channels and the plots of the time stamps of each spike during the designated time window on each active channel forms a raster plot. A raster plot allows a researcher to examine the temporal features and spatial features of SSA directly, regionally, or net-wide depending on how many active channels are selected. An active channel was defined to have five or more spikes per minute. The temporal features of SSA include the spike rate, burst rate, burst duration, inter-burst interval, inter-spike interval within a burst, and the rhythmicity of SSA etc.; the spatial features of SSA refer to the distribution of active channels, synchronicity or dis-synchronicity of spikes or bursts across active channels regionally or net-wide.

A total of 52 cultures from 9 dissections of E8-to-E10 forebrains were grown on MEA chips. Each batch of dissection generated 4-8 cultures on MEA chips. Half of the cultures in each batch were cultured in NB, and the other half in NB^+. One batch was plated at 1000 cells/mm^2, 2 batches at 1500 cells/mm^2, 4 batches at 2000 cells/mm^2, and 2 batches at 2500 cells/mm^2. SSA signals of these cultures were monitored frequently (often every other day) during the first three weeks of development. Like rodent counterpart, C-FBN-Cs were ready for acute neuroactive agent testing after three weeks and underwent a series of dose-response experiments. Results of dose-response experiments with selected classic neuroactive agents were reported earlier.[7] This paper deals with how long and how stable C-FBN-Cs lived in this condition, i.e., three weeks early development succeeded by repeated intervention of dose-response experiments. Some key results of the dose-response experiments are mentioned or summarized in the sections on Results and Discussion when necessary.

Results and discussion

Reduced plating density and serum-independency

In our previous study, C-FBN-Cs were maintained in $M199^+$.[10] To significantly prolong lifespan, plating density had to be as high as 3000 cells/mm^2; to maintain SSA throughout the culture's lifetime, M199 had to be supplemented with 10% FBS. The longest lifespan for E8 and E10 was one month, and 3 months for E12 cultures. Unlike our previous study, C-FBNs did better in NB and NB^+ than in $M199^+$: 1) The cells were able to survive and grow well in a reduced plating density ranging from 1000 to 2500 cells/mm^2; 2) they were able to survive and grow well in the absence of serum in NB and in the presence of a low level of serum (2% FBS) in NB^+. Interestingly, they did not tolerate a higher serum level; for example, when FBS was increased from 2% to 5%, cell monolayers detached from the MEA chip in about 3 days.

In addition, in our previous study[10] when $M199^+$ was used, E8, E10, and E12 cultures exhibited a remarkable embryonic age-dependent morphology. At the same cell plating density, the older the embryonic age, the lesser the cell aggregation, and the faster the culture became confluent. In this study, an embryonic age-dependent morphology was noticeable, but not obvious, for E8, E9, and E10 cultures. Furthermore, E12 cultures did not grow as well as E8-to-E10 cultures and tended to have compromised culture confluence, possibly due to cell degeneration. Therefore, E8-to-E10 cultures were used in this study.

Morphological features and stability of C-FBN-Cs

Culture morphology. Unlike E8 and E10 cells in $M199^+$ that formed aggregations (Fig. 1C) during the first week and did not easily reach confluence,[10] cells in NB did not aggregate (Fig. 1A); in NB^+, they aggregated to a small degree (Fig. 1B). In NB and NB^+, glial-cell proliferation was much faster than in $M199^+$, so cultures achieved confluence even with the reduced plating densities (1000 to 2500 cells/mm^2). Cultures in NB^+ achieved confluence one or a few days later than in NB due to slight cell aggregation (Fig. 1); this still was much faster than in $M199^+$ in our previous study. In NB and NB^+, after the culture became confluent, slight cell aggregation sometimes formed and was sparsely distributed in culture. These cell aggregations showed MAP2 positive staining, indicating that some neuronal somas tended to be gathered together (not shown). A confluent neuronal-glial co-culture was not a monolayer, but a thin 3D structure with layers of cells that could be observed by focusing on different depths of the culture under a phase-contrast microscope. In NB at 16 DIV, confocal microscopy 3D Z-stack images showed a culture thickness of about 11-13 μm except where neuronal somas clustered, where it was 18.8 μm. After confluence, cell loss was a very slow process, so morphological stability (100% confluence) could be maintained as long as 5 months. In comparison to our previous experience with $M199^+$, in which E8 and E10 cultures rarely achieved confluence and tended to detach from the MEA,[7] the location and the number of active channels of cultures in NB and NB^+ were more stable.

RSC Advances Accepted Manuscript

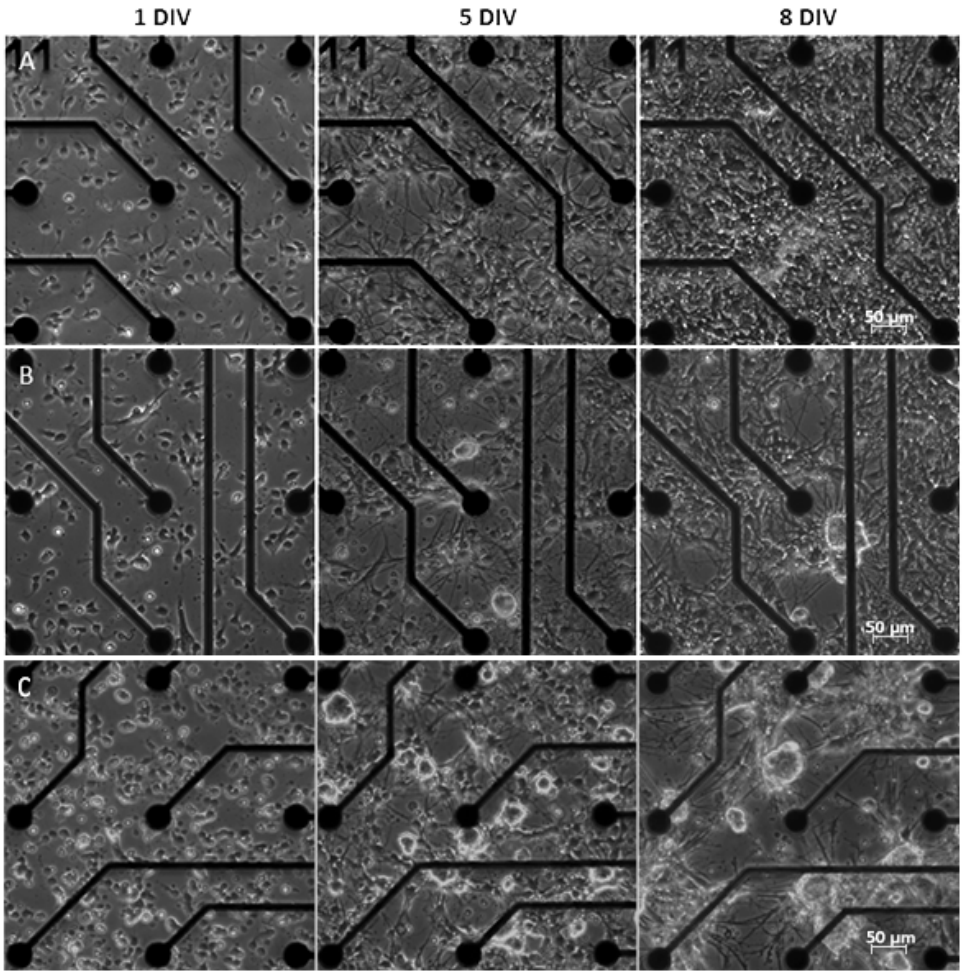

Fig. 1. A comparison of the culture morphology in NB (A), NB^+ (B) and $M199^+$ (C). Culture A and B were from same dissection and plated at the same density of 2000 cells/mm^2. We see rapid growth and confluence of culture A within a week and by just one or a few days' delay in culture B. Culture C in $M199^+$ was plated at 3000 cells/mm^2; cells formed clusters and the cell clusters increased in size along with time; not all cultures in $M199^+$ plated in this density can become confluent during their lifespan due to severe cell aggregation and relatively slow proliferation of glial cells.

Neurite morphology. Neurite morphology in NB was remarkably different from that in $M199^+$. A comparison of the two is shown in Fig. 2. Neurite morphology in NB can also be viewed clearly using immunostaining neuronal marker MAP2 (for soma and dendrites; Fig. 3A).

RSC Advances Accepted Manuscript

 This journal is © The Royal Society of Chemistry 2015

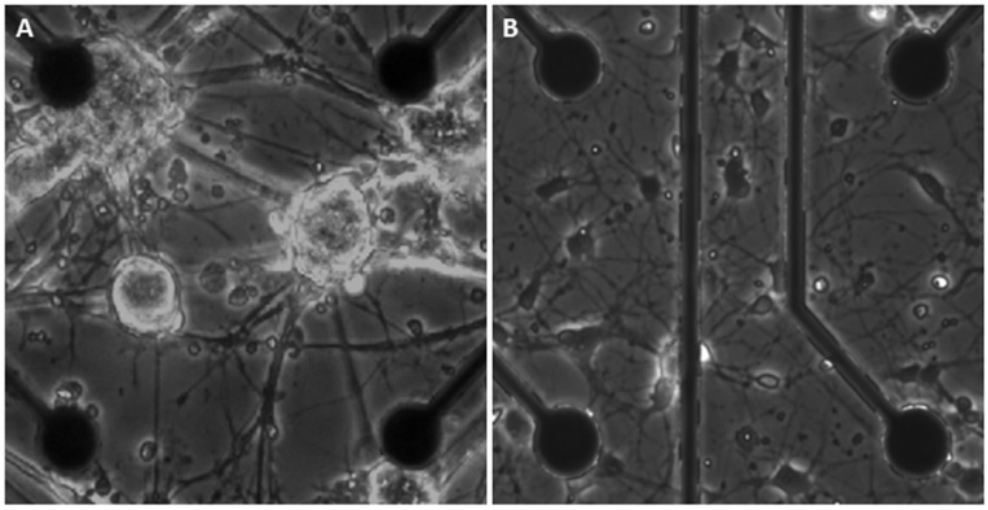

Fig. 2 Neurite morphology. A. Neurites in M199$^+$ were stretched due to cell aggregation and looked thick, possibly due to bundle formation; B. In contrast, neurites in NB were relaxed, abundant, and did not form bundles. Neurites in NB$^+$ looked similar to those in NB (not shown).

Confirmation of cell identities. We further confirmed cell identities by co-immunostaining the neuronal marker MAP2 and the astrocyte-specific glial cell marker GFAP (Fig. 3).

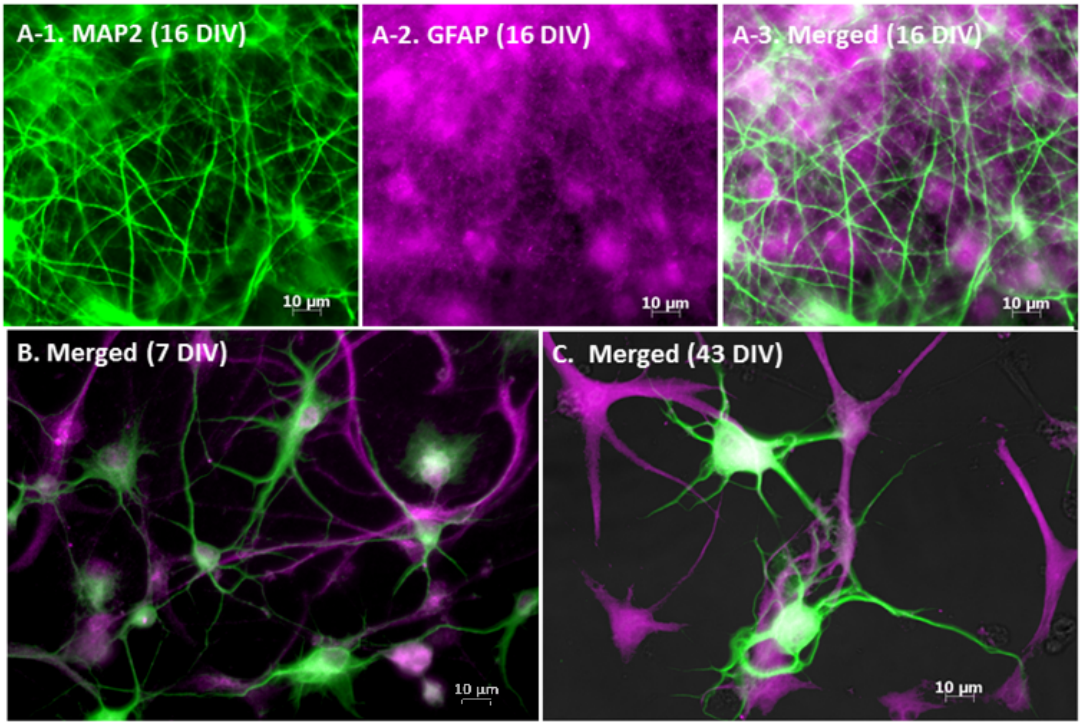

Fig. 3 Phase-contrast images (40x) show results of MAP2 (green) and GFAP (magenta) co-staining for cultures at three different DIVs. A. In a 16 DIV culture (2000 cells/mm^2, 3A, 3B, and 3C), glial cells filled the spaces within the neuronal network, making individual glial cells difficult to see and indicating fast glial proliferation in NB. To show typical astrocytes, a relatively sparse culture (1000 cells/mm^2) was co-stained at 7DIV (B); another culture (1000 cells/mm^2), co-stained at 43 DIV, in which neurites had undergone degeneration, but astrocytes typically appeared (C).

In contrast to cultures in M199$^+$ in our previous study,[10] the fast glial proliferation and thus the fast confluence of a culture in NB or NB$^+$ as shown in Fig. 1 and Fig. 3A were desirable. We believe this rapidity 1) was the major contributor toward the 5-month morphological stability of C-FBN-Cs achieved in this study; and 2) ensured the long-term functional stability reported below.

Functional features and stability of C-FBN-culture

RSC Advances Accepted Manuscript

General development of SSA. In both NB and NB$^+$, the earliest time-point at which spikes emerged was 4 DIV, the same as in M199$^+$.[10] The active channel count (ACC, i.e., number of active channels) increased rapidly during the first week, reached its maximum in the second week, and levelled off slightly after the second week; ACC in some cultures may increase again gradually after three weeks, and most cultures ended up with a total ACC in a range from 15 to 50. The rate of ACC increase depended on neuronal density, dissection batch, and presence of 2% FBS. During development, spikes at active channels gradually self-organized into bursts. Bursts at active channels fired simultaneously to form network-wide synchronized bursts (Fig. 4A), known as "population bursts," [10, 14] which indicate a highly coordinated, efficient network-wide synaptic transmission. The same or similar patterns of population burst recurred rhythmically (Fig. 4B). The characteristic firing pattern of SSA from C-FBN-Cs is recurrent, rhythmic, synchronized network-wide population burst events that exhibit a high spatiotemporal coherence in their structure. In this, C-FBNs are similar to their rodent counterpart. In addition to this characteristic pattern (population bursts) of SSA, a different pattern of SSA, channel-self firing rhythms, often occurred in a very small fraction of ACC, which is described below and in the caption of Fig. 4B.

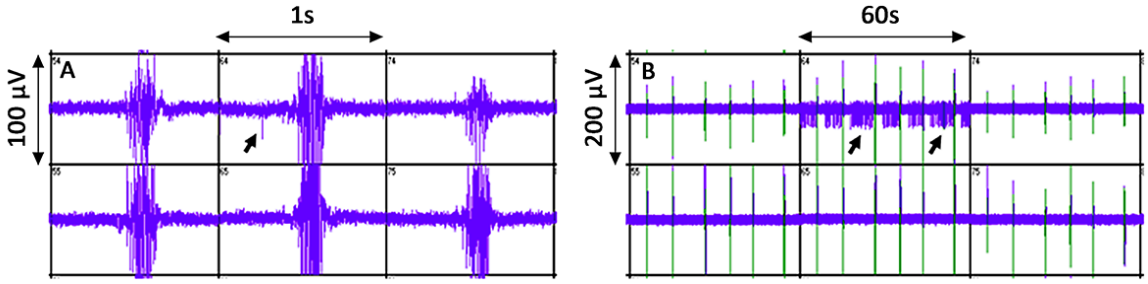

Fig. 4 Direct screenshots of population bursts and channel-self rhythm (from MC_Rack); 6 active channels. Bursts in individual channels occurred simultaneously to form typical population bursts in the 1-second-window view (A). Similar patterns of population bursts recurred rhythmically and appear as vertical bars in the 60-second window (B). Arrows in both A and B indicate unsynchronized channel-self rhythms that were often faster than the rhythm of population bursts. Spikes with this rhythm often fired with smaller amplitudes. When the spike-detection threshold was set below the amplitude of these spikes that are nonsynchronized with the population bursts, only spikes within population bursts were detected. MC_Rack automatically shows detected spikes with a green color and undetected signals with a blue color. To make it easy to see the green lines, the blue signals were modified to be purplish as seen in B.

Properties of population bursts. Several distinct properties of population bursts were observed (in this paper and in previous publications) and were summarized as follows: 1) Regularity—rhythmicity in time and high synchronicity in space across active channels (Fig. 4). 2) Stability—regularity of population bursts can be maintained up to 5 months in C-FBN-Cs (Fig. 5)—this is the functional stability of SSA C-FBN-Cs can achieve in current culture settings (NB and NB+). 3) Tissue specificity—similar to findings in the rodent counterpart, this feature can be clearly seen when compared with firing patterns from a cultured network formed by spinal cord neurons and was reported in our previous paper.[10] 4) Great variation in rhythm—each culture's population bursts had their own oscillatory rhythm. The range of rhythms for each culture was very large; this allowed the dose-response experiments for neuroactive chemicals to be conducted within a broad log10[dose] range.[7] Rhythms between sister cultures from the same dissection could be similar or quite different. 5) Dose-dependent responsiveness to classic neuroactive agents.[7] Fig. 5 shows two sets of raster plots of two cultures from different dissections (Fig. 5A and 5B). Culture A was maintained in NB without being exposed to classic neuroactive agents. Culture B was maintained in NB+ and underwent repeated dose-response experiments using a variety of classic neuroactive agents. Both cultures showed approximately 5-month-long functional stability (regularity of population bursts). Variations in their oscillation rhythms can also be seen (Fig. 5).

RSC Advances Accepted Manuscript

 This journal is © The Royal Society of Chemistry 2015

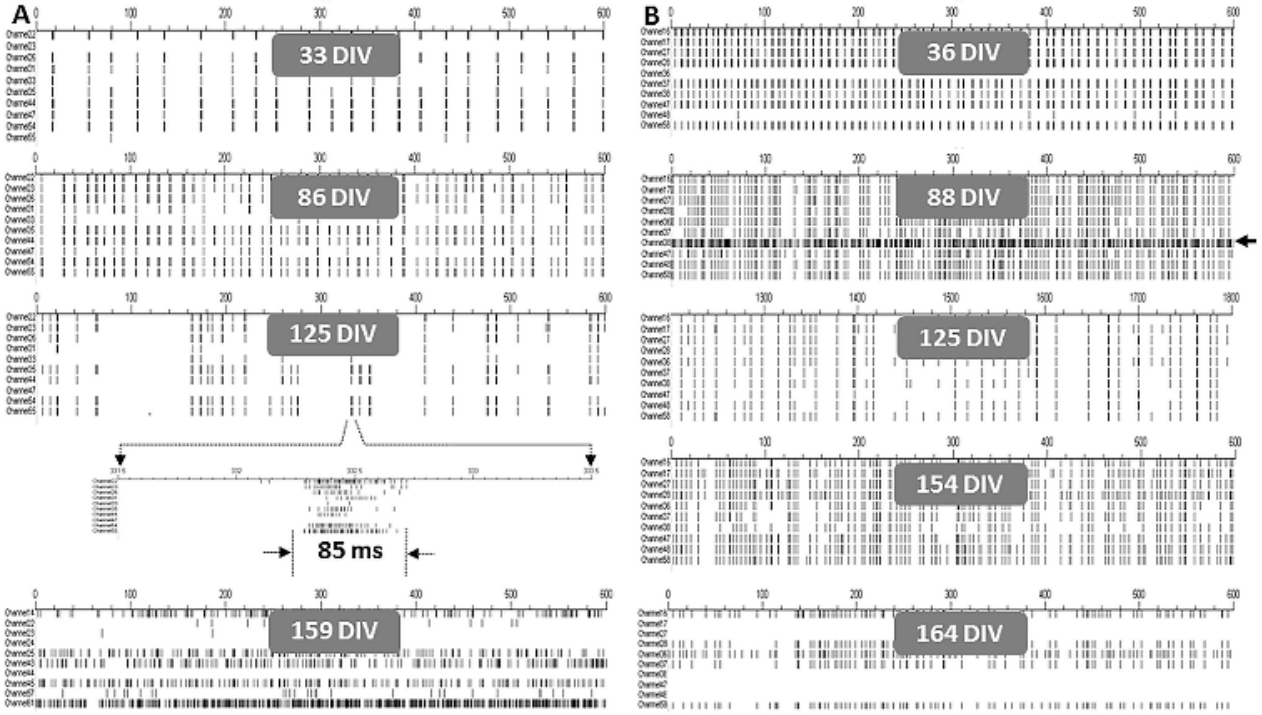

Fig. 5 Selected raster plots from Cultures A and B with ten representative channels at different DIVs recorded for 600 seconds. Population burst regularity, long-term stability, and rhythmic variations are shown and can be compared between Culture A and Culture B, excepting the last raster plot for each culture (A-159 DIV and B-164 DIV). These last two raster plots show typical features of late SSA after about 5 months when cultures underwent a slow aging process: 1) gradual loss of spatial synchrony of population bursts, exemplified in A-159 DIV; 2) tendency of remaining active channels to fire at a much faster rate, exemplified in A-159 DIV; and/or 3) significant loss of active channels, exemplified in both raster plots. As a culture ages, these three features may occur together or serially. The ten representative channels in A-159 DIV and B-164 DIV were slightly different from the ten channels that were same for all other raster plots above each respectively, showing these three features that characterize late SSA. These two sets of raster plots demonstrate the lifespan of C-FBN-C with robust SSA in both NB and NB^+. Furthermore, the regularity and stability of population bursts are well-maintained within 5 months.

Individual channel-self rhythm. In contrast to the population bursts with regularity in space and time as the dominant pattern of SSA, some channels in some networks showed a channel-specific firing rhythm (Fig. 4A and 4B, Fig. 5B-88DIV). These channel self-rhythms occurred in only a small fraction of ACC, might or might not synchronize with some neighbor channels, were often much faster than the rhythms of population bursts, often showed smaller magnitude than population bursts, could fire tonically or intermittently, and could persist (as long as population bursts) for the short-term (a few days), or transiently (seconds-to-minutes). Persistent individual channel self-rhythm occurred natively in a very few (often one or two) channels for some cultures. This type of channel-self rhythm persisted and could be lifelong. In contrast, short-term and transient channel-self rhythms often occurred in more than two channels after an environmental perturbation to a culture, such as change of medium, neuroactive-agent administration or withdrawal, or injection of CO_2 into the cell-culture incubator. Thus, short-term and transient channel-self rhythm seems to indicate a temporal mechanical disturbance a culture was experiencing or experienced. The spikes and bursts within population bursts responded dose-dependently to neuroactive agents. So in dose-response experiments, by setting a relatively lower spike detection threshold, channel-self rhythms can be effectively excluded (Fig. 4B).

In brief, population bursts were network-wide, long-lasting, robust, and relatively stable, reflecting a network's functional integrity and stability. In contrast, channel-self rhythms were either specific to individual channels or involved a few neighboring channels regionally, brief in most cases, and changeable.

Late SSA in C-FBN-Cs. Regularity of population bursts in space and time was gradually and slowly compromised; this usually occurred after 4-5 months, depending on cell densities and different batches. Synchronous active channels were reduced or disappeared, and remaining active channels fired much faster than the synchronized rhythm of population bursts (Fig. 5A-159 DIV). Sometimes in a late stage, with a gradual loss of the area that covered the electrodes, the number of active channels decreased dramatically, but the regularity of population bursts continued in these few active channels (Fig. 5B-164 DIV). In general, the degeneration of C-FBN-Cs was a slow, progressive process.

SSA enhancement in the presence of 2% FBS. How serum affects SSA has not been specifically studied in MEA-based rodent neuron biosensors. A wide range of serum concentration (from 0 to 10% or more) and sera from various animals (fetal bovine, calf, and horse etc.) have been used.[15-17] We observed a notable SSA-enhancing effect for cultures in NB^+ in comparison to cultures in NB. It was repeatable and consistent in all batches of cultures used in this study. Fig. 6 shows a comparison of representative screenshots of SSA in NB and NB^+ respectively at 2 different DIVs. This SSA-enhancing effect in the presence of 2% FBS can also be seen in Fig. 7.

RSC Advances Accepted Manuscript

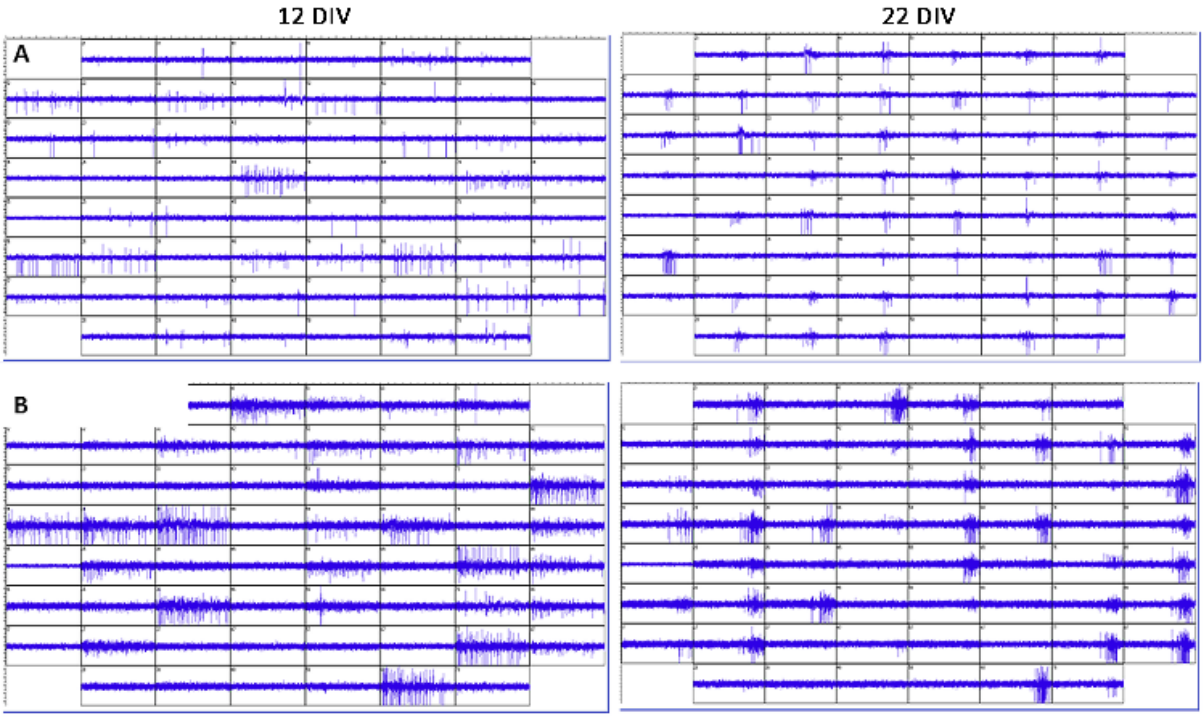

Fig. 6 Screenshots of SSA at 12 DIV and 22 DIV from sister cultures dissected on the same day and plated at the same cell density. A. Signals from the NB culture; B: signals from the NB$^+$ culture. Although the cultures had different noise levels, it is still obvious that culture B had more spikes on its active channels at 12 DIV than culture A, and its bursts were more densely packed at 22 DIV than in culture A.

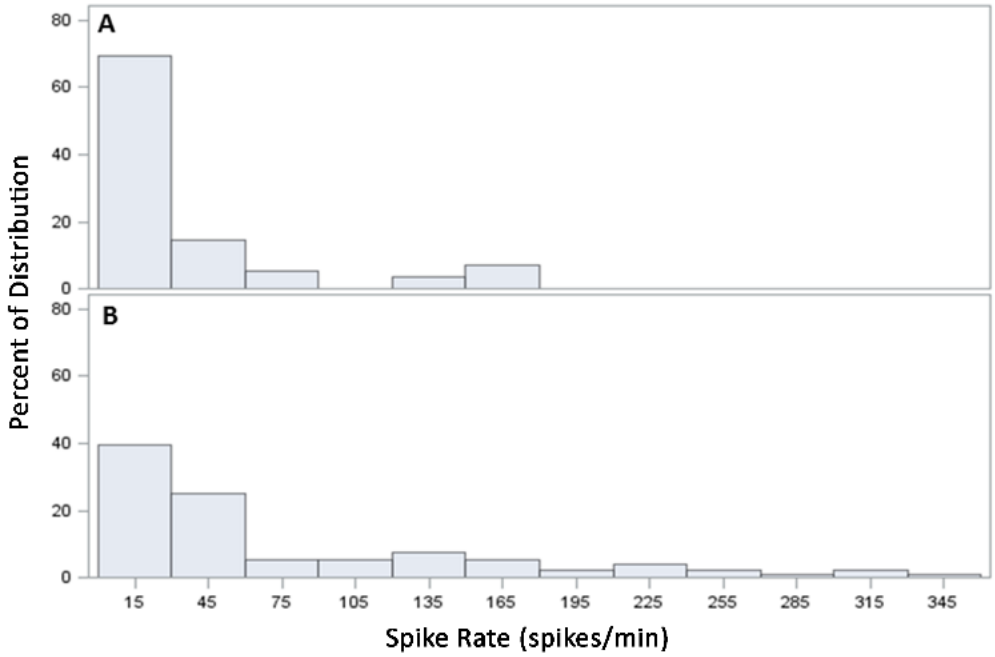

Fig. 7 A comparison of spike rate distribution at 12 DIV between sister cultures plated at the same density (A, NB; B, NB$^+$). The distribution of SR in both NB and NB$^+$ were left-skewed. The highest SR at 12 DIV for NB group is at 165 spikes/min; the highest SR for NB$^+$ group is up to 345 spikes/min. This left-skewed distribution pattern for SR was consistent from 6 DIV to 22 DIV; SR from the NB$^+$ group always occurred at a region where SR was much higher than that from the NB group. Burst rate (BR) distribution showed a similar left-skewed pattern and a similar degree of difference between NB and NB$^+$ groups (not shown).

RSC Advances Accepted Manuscript

Table 1 presents the results of significance tests using the non-parametric two-sample Wilcoxon method for median spike rate comparison respectively at each recorded DIV (except 4 DIV due to too small sample size) during the first three weeks. The differences between the two medians were all significant with a one-tailed *p*-value much less than 0.05 from both groups from the same dissection.

Table 1. A comparison of median spike rate between NB group and NB^+ group during the first three weeks of C-FBN-C development using Wilcoxon test (ACC: active channel count from 3 MEAs; *: One-Tailed p-value)

DIV	Sample Size (Total ACC)		Median SR (Spikes/min)		Statistical Test between NB and NB^+		
	NB	NB^+	NB	NB^+	Wilcoxon Statistic	*p*-value*	Significance
6	26	55	16.65	21.72	1.9272	0.027	yes
8	34	89	11.3	41.11	6.0709	0	yes
10	58	111	24.2	66.97	6.4354	0	yes
12	56	96	20.65	36.16	3.4204	0.0003	yes
14	49	71	17.2	26.16	1.9755	0.0241	yes
16	52	71	15.15	29.9	4.0165	0	yes
18	63	63	18.8	54	5.3623	0	yes
20	56	47	14.25	59.09	6.2471	0	yes
22	51	45	13.86	92.04	7.0852	0	yes

Lifespan of more than 5 months for C-FBN-Cs

In this study, unlike our previous one,[10] the lifespan of C-FBN-Cs using NB and NB^+ was comprehensively evaluated using 52 cultures from 9 dissections of E8-to-E10 forebrains plated at a range of cell densities (1000 to 2500 cells/mm^2) with repeated interventions using classic neuroactive agents (dose-response experiments).

Typically, an acute dose-response experiment lasted 5-7 hours depending on the neuroactive agent tested and the number of doses administered. Following the experiment, the culture was washed 3 times in fresh medium and maintained in fresh medium. The time window for conducting dose-response experiments was 21 DIV to 139 DIV. The minimum interval between two acute dose-response experiments was 4 days. The maximum number of repeated dose-response experiments conducted on a single culture was 14 times. Under such circumstances, unlike our cultures maintained in $M199^+$,[8] detachment of the culture from the MEA surface in NB and NB^+ occurred much less frequently. Moreover, most C-FBN-Cs in both NB and NB^+ maintained their morphological and functional stability for more than 4 months as long as the medium osmolarity and pH were carefully managed; the longest period of stability in morphology and function was 5 months (Fig. 5B-154 DIV).

After 5 months, the morphological and functional stability of C-FBN-Cs were gradually compromised and replaced with features of late SSA, suggesting an aging process. However, C-FBN-Cs were still spontaneously active for up 7 months. We find that 1) like their mammalian counterparts, C-FBN-Cs were well-suited to NB and NB^+ and 2) C-FBN-Cs achieved a lifespan of more than 5 months with their morphological and functional stability well-maintained for 5 months.

Reports about the lifespan of rodent counterparts do not provide information about how lifespan was determined or whether cultures maintained morphological and functional stability. Reported lifespan varies from weeks to more than 9 months.[12, 18-23] Here, we report prolonging the lifespan of C-FBN-cultures from the previously reported maximum of 14 days to a length similar to that of rodent counterparts. In summary, the results presented above have demonstrated that C-FBN-Cs can be successfully established on the MEA platform with more than 5 month-long lifespan and up to 5 month-long stability in morphology and function.

Pros and cons of chick FBNs as a source of MEA biosensor

C-FBN-C vs. rodent counterpart. 1) Based on findings in this paper, combined with our data of pharmacological characterization using selected classic neuroactive agents in a previous publication,[10] C-FBN-C on MEA forms a useful C-FBN-biosensor system of its own type and can be used widely for research in the fields of electrophysiology, neuroscience, biology, pharmacology, and neurotoxicology for avian species as well as for comparative biology across species. 2) It is reasonable that we observed remarkable functional similarity in terms of the overall spatial and temporal patterns of SSA, tissue specificity, and responsiveness to selected classic neuroactive agents between C-FBN-C and rodent counterpart, because no matter how differently the cortical tissues are organized and wired, when cortical tissues from the two species are dissociated and new in vitro neuronal networks are formed in cell culture from these dissociated neurons, chances to see functional similarity increase due to shared neocortical input and output neurons.[9] However, there must be differences in the in vitro neuronal networks between the two species that we have not discerned in our current experimental setting and with limited known neuroactive agents. More pharmacological characterization work needs to be done to know more about the similarities and differences (shared and not-shared functional domains such as the types and subtypes of ligand-gated receptors expressed in the cultures) of the in vitro networks between the two species. 3) Knowing shared and not-shared functional domains is of particular value to cope with a long-standing, pressing demand for a rapid, screening-based approach to assessing numerous neurotoxic substances in the environment due to severe pollution, which has been correlated to the rapid increase in the rate of occurrence of a series of neurodevelopmental disorders.[24-27] The European Commission's Regulation on Registration, Evaluation, Authentication and Restriction of Chemicals has estimated a cost of about 3 million test animals to test approximately 30,000 existing substances.[28, 29] Although rodent neuron biosensor

RSC Advances Accepted Manuscript

has shown its ability for rapid, sensitive, functional screening of neurotoxic substances, the scale of testing, the European Commission's advocacy of reducing animal use, and the cost of rodents (about $250 per pregnant female rat; about $30 per regular rat; a bit more than $100 per pair of commercially available cryopreserved rat cortex) limit application of rodent neuron-based MEA biosensors. If many shared functional domains can be discovered between the two species and major functional differences become known, chick-FBN biosensor may hold the potential to be used as an alternative screening approach within shared functional domains as a very economic and convenient tool (about $1 per egg). 4) Rodent counterpart has also been used in assessing the sub-chronic neurotoxicity of substances.[30] With 5-month-long stability of C-FBN-C, it also has the potential to be used for the same purposes. 5) From our previous work using M199^{+} [10] and this paper, we learned that glial cells play an important role in the development of in vitro neuronal networks and the functional stability of SSA. However, the growth and proliferation of glial cells need to be characterized, and the C-FBN-Cs have the potential to play a role in the study of neuron-glia interaction.

C-FBNs vs. hiPSCs. Human safety risks of substances with nervous system effects are conventionally evaluated using data from animal models and in vitro assays on related animal tissues or cells. The inter-species differences limit the value of this approach. The availability of the technology to generate hiPSCs from mature human cell sources[5] has opened a new and promising field for neurotoxin assessment.[6] The unreplaceable advantages of hiPSCs are that 1) they are human cells, which avoids the limitation mentioned above; 2) they have the potential to be a large or even unlimited source of human cell supply; 3) theoretically, they can potentially be induced to differentiate into particular cell types according to the need and the purpose of research; 4) technically, some cell types induced from hiPSCs are now commercially available;[6] and 5) there is no need to do tissue dissection. Regarding human safety issues, C-FBNs do not have these advantages that hiPSCs have. Regarding animal biology and comparative biology, the indication or the sphere of application of the two cell sources do not overlap. Moreover, hiPSCs generate populations of specific types of cell, whereas C-FBN-C as well as rodent counterpart are natural mixes of all types of neurons and glial cells from forebrain tissue or rodent cortex. Hence, they basically serve the needs for neurotoxicity assessment at different levels: hiPSC is more suitable for cell type-specific toxicity assays, whereas C-FBN-Cs and rodent counterpart are for cortical tissue-specific toxicity assays. Before hiPSCs can be readily and cost-effectively delivered as a routine screening for neurotoxins, significant work is required to ensure accurate mature cell phenotypes, high yields, and the ability to maintain their differentiated phenotypes for extended periods. hiPSCs also hold the potential to be technically and economically differentiated into certain tissue types with mixed types of cells, however, it will take a longer time and more complicated procedure to achieve this point than to produce a single cell type-specific neuron supply, while C-FBN-Cs have been successfully, conveniently, and cost-effectively established on MEA and are ready for multiple usage.

Conclusions

This paper shows evidence that a 5-month long-term stable C-FBN-C can be established on MEA platform and that it is well-suited to NB and NB^{+} designed for rodent neuron cultures. Combined with our data on the pharmacological characterization of the C-FBN-Cs,[7] this technique is of value to be widely used in the areas of electrophysiology, neuroscience, biology, pharmacology, toxicology, and comparative physiology. It also has the potential to be used conveniently and cost-effectively in very large-scale environmental neurotoxicant screening within the shared functional domains with rodent counterpart to help deal with the long-standing and pressing demand for an economical functional assessment tool for neurotoxicity.

Acknowledgements

This work was partially supported by funding from the National Institutes of Health through SC COBRE (P20RR021949), the National Natural Science Foundation of China (No. 31070847 and 31370956), the Strategic New Industry Development Special Foundation of Shenzhen (No. JCYJ20130402172114948), and Guangdong Provincial Department of Science and Technology, China (2011B050400011).

References

1 A.F. Johnstone, G.W. Gross, D.G. Weiss, O.H. Schroeder, A. Gramowski, and T.J. Shafer, *Neurotoxicology*, 2010, **31,** 331. DOI: 10.1016/j.neuro.2010.04.001
2 L. Ylä-Outinen, J. Heikkilä, H. Skottman, R. Suuronen, R. Aänismaa, and S. Narkilahti, *Frontiers in Neuroengineering,* 2010, **3.** DOI: 10.3389/fneng.2010.00111
3 I. Laurenza, G. Pallocca, M. Mennecozzi, B. Scelfo, D. Pamies, and A. Bal-Price, *International Journal of Developmental Neuroscience,* 2013, **31,** 679.
4 M. Chiappalone, A. Vato, M. B. Tedesco, M. Marcoli, F. Davide, and S. Martinoia, *Biosensors and Bioelectronics,* 2003, **18,** 627.
5 K. Takahashi, K. Tanabe, M. Ohnuki, M. Narita, T. Ichisaka, K. Tomoda, and S. Yamanaka, *Cell,* 2007, **131,** 861.
6 C.W. Scott, M.F. Peters, and Y.P. Dragan, *Toxicology Letters,* 2013, **219,** 49.
7 S.Y. Kuang, Development and characterization of chick forebrain neuron-based neurotoxin biosensor on a microelectrode array [Dissertation], 2014. Clemson University, South Carolina, USA
8 R. Tokioka, A. Matsuo, K. Kiyosue, M. Kasai, and T. Taguchi, *Developmental Brain Research*, 1993, **74**, 146.
9 J. Dugas-Ford, J.J. Rowell, and C.W. Ragsdale, *Proceedings of the National Academy of Sciences,* 2012, **109,** 16974.
10 S.Y. Kuang, Z. Wang, T. Huang, L. Wei, T. Xi, M. Kindy, and B.Z. Gao, *Biotechnology Letters*, 2015, **37,** 499. DOI: 10.1007/s10529-014-1704-1
11 S.R. Heidemann, M. Reynolds, K. Ngo, and P. Lamoureus, *Methods in Cell Biology,* 2003, **71,** 51.
12 S.M. Potter and T.B. DeMarse, *Journal of Neuroscience Methods*, 2001, **110**(1-2), 17.
13 G.J. Brewer, E.K. Torricelli, and P.J. Price, *Journal of Neuroscience Research*, 1993, **35**, 567.
14 V. Pasquale, P. Massobrio, L.L. Bologna, M. Chiappalone, and S. Martinoia, *Neuroscience*, 2008, **153,** 1354. DOI: 10.1016/j.neuroscience.2008.03.050
15 A. Novellino, B. Scelfo, T. Palosaari, A. Price, T. Sobanski, T. J. Shafer, A.F. Johnstone, G.W. Gross, A. Gramowski, O. Schroeder, K. Jugelt, M. Chiappalone, F. Benfenati, S. Martinoia, M.T. Tedesco, E. Defranchi, P. D'Angelo, and M. Whelan, *Frontiers in Neuroengineering,* 2011, **4**(4). DOI: 10.3389/fneng.2011.00004
16 B.L. Robinette, J.A. Harrill, W.R. Mundy, and T.J. Shafer, *Frontiers in Neuroengineering*, 2011, **4**, 1. DOI: 10.3389/fneng.2011.00001
17 A. Gramowski, K. Jügelt, O.H. Schröder, D.G. Weiss, and S. Mitzner, *Toxicological Science*, 2011, **120**(1), 173. DOI: 10.1093/toxsci/kfq385
18 F. Otto, P. Görtz, W. Fleischer, and M. Siebler, *Journal of Neuroscience Methods*, 2003, **128**(1-2), 173.
19 S. Martinonia, L. Bonzano, M. Chiappalone, M. Tedesco, M. Marcoli, and G. Maura, *Biosensors and Bioelectronics*, 2005, **20**, 2071.
20 G. Xiang, L. Pan, L. Huang, Z. Yu, X. Song, J. Cheng, W. Xing, and Y. Zhou, *Biosens Bioelectron*, 2007, **22**, 2478.
21 A. Novellino, B. Scelfo, T. Palosaari, A. Price, T. Sobanski, T. J. Shafer, A. F. Johnstone, G. W. Gross, A. Gramowski, O. Schroeder, K. Jugelt, M. Chiappalone, F. Benfenati, S. Martinoia, M.T. Tedesco, E. Defranchi, P. D'Angelo, and M. Whelan, *Frontiers in Neuroengineering*, 2011, **4**(4). DOI: 10.3389/fneng.2011.00004

RSC Advances Accepted Manuscript

 This journal is © The Royal Society of Chemistry 2015

22 V. Magloire, A. Czarnecki, H. Anwander, and J. Streit, *Neuroscience*, 2011, **172**, 129. DOI: 10.1016/j.neuroscience.2010.10.034
23 Y. Xia and G. W. Gross, *Alcohol*, 2003, **30**(3), 167.
24 L.R. Goldman and S. Koduru, *Environmental Health Perspectives*, 2000, **108**(suppl 3), 443.
25 United States Environmental Protection Agency, *Chemical hazard data availability study: what do we really know about the safety of high production volume chemicals?* Washington, DC: Office of Pollution Prevention and Toxics, 1998.
26 M. Kajta and A. Wójtowicz, *Przeglad Lekarski,* 2010, **67**, 1194.
27 National Environmental Trust, *Polluting our future: chemical pollution in the U.S. that affects child development and learning,* 2000. Available from http://grconnect.com/reports/pollutingourfuture.pdf
28 A.K. Bal-Price, C. Sunol, D. G. Weiss, E. van Vliet, R.H. Westerink, and L.G. Costa, *Neurotoxicology,* 2008, **29**(3), 520. DOI: 10.1016/j.neuro.2008.02.008
29 T. S. Hartung, S. Bremer, S. Casati, S. Coecke, R. Corvi, S. Fortaner, L. Gribaldo, M. Halder, A. J. Roi, P. Prieto, E. Sabbioni, A. Worth, and V. Zuang, *Alternatives to Laboratory Animals*, 2003, **31**(5), 473.
30 K.V. Gopal, B.R. Miller, and G.W. Gross, *Journal of Neural Transmission,* 2007, **114,** 1365.

RSC Advances Accepted Manuscript